Alternative EEG pre-processing pipelines can lead to conflicting conclusions regarding cortical excitation/inhibition ratio

Frigyes Samuel Racz[1,2*], Diego Mac-Auliffe[1,3], Peter Mukli[4,5], John Milton[1], Juan Luis Cabrera[6,7], José del R. Millán[1,2,3]

[1]Department of Neurology, The University of Texas at Austin, 1601 Trinity Street, Austin, 78712, Texas, United States.
[2]Mulva Clinic for the Neurosciences, The University of Texas at Austin, 1601 Trinity Street, Austin, 78712, Texas, United States.
[3]Chandra Family Department of Electrical and Computer Engineering, The University of Texas at Austin, 2501 Speedway, Austin, 78712, Texas, United States.
[4]Oklahoma Center for Geroscience and Healthy Brain Aging, University of Oklahoma Health Sciences Center, 1100 N Lindsay Ave, Oklahoma City, 73104, Oklahoma, USA.
[5]Vascular Cognitive Impairment and Neurodegeneration Program, University of Oklahoma Health Sciences Center, 1100 N Lindsay Ave, Oklahoma City, 73104, Oklahoma, USA.
[6]Centro de Física, Instituto Venezolano de Investigaciones Científicas, Caracas, 1020-A, Venezuela.
[7]Departamento de Física Aplicada, ETSI Aeronáutica y del Espacio, Universidad Politécnica de Madrid, Pza. Cardenal Cisneros 3, Madrid, 28040, Spain.

*Corresponding author(s). E-mail(s): fsr324@austin.utexas.edu;

Abstract

Confluent recent evidence indicates that the spectral slope of $\mathbf{1/f}$ neurophysiological recordings is correspondent to cortical excitation/inhibition (E/I) ratio. In this framework, a steeper power spectrum (i.e., one with a larger spectral exponent $\boldsymbol{\beta}$) is indicative of stronger inhibitory tone and thus lower E/I ratio, and vice

versa. While the tools commonly utilized for estimating $\boldsymbol{\beta}$ are mostly consistent, there appears to be a lack of standardization among data processing protocols for slope analysis. In this work our goal is to draw attention to a fundamental consequence of this issue, namely that even in a confined, comparative research environment, applying different pre-processing steps to electroencephalography (EEG) data can lead to conflicting conclusions in terms of the E/I ratio. To this end, we analyzed resting-state EEG recordings in two independent datasets, containing data collected with eyes open (EO) and eyes closed (EC), with the latter considered as a physiological state with stronger inhibitory tone. Our analysis confirmed consistently in both cohorts that applying different spatial filtering schemes in an otherwise identical analytical pipeline indicated a decrease in E/I ratio over the prefrontal cortex in one case, but not the other when transitioning from EO to EC. In contrast, this same pattern was apparent over the occipital cortex regardless of the pre-processing scheme. This empirical evidence calls for the development of a standardized data processing protocol for EEG-based analyses of the E/I ratio.

Keywords: E/I ratio, spectral slope, $\mathbf{1/f}$, spatial filtering, EEG

1 Introduction

It is well established that brain activity is characterized with a $1/f$-type power spectrum, indicating a scale-free or *fractal* nature of neural dynamics [1, 2]. In that, spectral power $|A(f)|^2$ of sampled neural activity follows a power-law dependency on frequency and the scale-free property is characterized via the spectral exponent β according to $|A(f)|^2 \propto cf^{-\beta}$ with some constant c [3]. Notably, when the power spectrum is visualized on a log-log scale, β is equivalent to the coefficient of an ordinary least squares (OLS) regression model and thus it is also often referred to as the *spectral slope* [4]. Despite being the focus of interest for decades now, however, the exact origin of $1/f$ scaling is not yet fully understood. Buzsaki and Draghun [5] proposed that this property emerges from the spatio-temporal integration of oscillatory activities from neuronal populations of varying size. Other works attempted to explain the emergence of $1/f$ scaling based on synaptic currents and membrane leakage properties [6]. It has been proposed lately that the spectral slope of local field potentials (LFP) indeed reflect the ratio of incoming excitatory and inhibitory activity (E/I ratio) to a given region [7]. According to this hypothesis, a steeper slope (i.e., higher absolute value of β) indicates an increase in inhibitory tone, while the opposite holds for an increase in excitatory input. This, combined with recent methodological advances for estimating β from empirical data [4, 8] resulted in a renewed interest in investigating scale-free brain activity and its physiological relevance. In line, several independent works provided support for the E/I ratio hypothesis via pharmaceutical interventions [9–11], optogenetics [12] or computational modeling [13]. In spite of the wide recognition of the E/I ratio hypothesis and the growing body of confluent evidence, however, this late resurgence of research activity brought a number of issues to light that need to be addressed.

First, it has been reported consistently that power spectra of neurophysiological data express *multimodality* i.e., the spectrum can be divided into multiple frequency regimes with different scaling exponents [6, 9, 14, 15]. In case of electrocorticogram (ECoG) and electroencephalogram (EEG) recordings, this manifests mostly as a *bimodal* nature in the 1-80 Hz range, where the two different — low- and high-frequency — scaling regimes are roughly separated by the alpha peak at about $\sim$10 Hz [4, 14, 15]. Apart from a few exceptions [9], most recent studies did not take this multimodality into consideration and instead characterized the broadband (e.g., from 1 to 45 Hz) spectrum with a singular β, or limited their analyses to a narrow frequency range where the spectrum can be considered unimodal. This bimodality, however, can have a seminal effect on how estimates are interpreted in the context of E/I ratio. Becker and colleagues [16] reported that spectral slope in the low-frequency regime ($<$ 5 Hz) reduces with the increase of inhibitory tone. This might appear contradictory to the model of Gao et al. [7], yet it must be stressed that they only claimed validity of the E/I ratio hypothesis in the 30-50 Hz regime, as well as Becker and coworkers took resting alpha power as a proxy for inhibitory tone, based on the "Gating by inhibition" hypothesis of Jensen and Mazaheri [17]. On the other hand, after administering Tiagabine — a GABA agonist increasing inhibitory tone —, Muthukumaraswamy and Liley [9] reported a simultaneous decrease in low-range slope β_{lo} (in line with [16]) and increase in high-range slope β_{hi} (in line with [7]). These results rather suggest that low- and high-frequency activity relate to E/I ratio in an opposite manner, and thus the power spectrum of neural data should be treated as bimodal.

Another crucial aspect that warrants attention is the lack of a standardized pre-processing pipelines for slope analysis in EEG-based studies. Even in the seminal paper of Gao and coworkers, the Authors advised that *"slope-inferred E:I ratio should only be interpreted in the context of a comparative experimental design in which the relative E:I ratio can be interrogated in response to experimental manipulations or population differences"* [7], as many factors might influence slope estimates including reference scheme, ambient noise or data processing steps [18]. This not only poses a major limitation on the comparability of outcomes reported by independent studies — thus reducing the potential of the spectral slope as a clinically relevant biomarker —, but it can have severe impact on how study outcomes are interpreted in terms of the E/I ratio hypothesis. In fact, several, commonly utilized data processing steps - such as re-referencing or spatial filtering schemes - can introduce an effect on the power spectrum (and thus spectral slope estimates) that can be quantified based on mathematical principles. Despite the importance and far-reaching implications of this issue, to the best of our knowledge it has not been explicitly and systematically investigated previously, which is particularly relevant considering the recently growing interest in slope-based analysis. In this work our goal is to take the first step towards filling this knowledge gap by demonstrating that variations of the analysis pipeline can have a fundamental effect on outcomes — and thus conclusions — even within a confined, comparative single study environment.

Precisely, our goal is to systematically investigate, how spectral slope estimates are affected by applying different pre-processing steps to EEG data, and if this can affect study conclusions when outcomes are interpreted in the framework of E/I ratio.

To this end, we employ the following simple experimental environment and considerations. Eyes-closed (EC) compared to eyes-open (EO) resting-state is characterized by a generalized increase of alpha synchronization that is most prominent over the occipital cortex [19]. If we accept the same assumption as Becker and colleagues [16] in that stronger alpha power indicates more prominent inhibitory tone/lower E/I ratio [20], then we can consider switching from EO to EC as a trivial case of physiological intervention, where EC is a state characterized by stronger inhibition compared to EO (lower E/I ratio), which in turn represents increased excitatory tone (higher E/I ratio). In a confined experimental design, we investigate the activity over two cortical locations — a prefrontal and a parieto-occipital one —, hypothesizing a more prominent increase in inhibitory tone in EC over occipital compared to frontal regions based on known spatial characteristics of resting-state EEG [19]. Namely, we assume that closing the eyes will increase inhibition (decrease E/I ratio) over the occipital cortex but not — or only to a lesser extent — over the prefrontal cortex. In line with previous literature on EEG spectra bimodality [6, 9, 14, 15], we analyze spectral slopes for low- and high-frequency regimes separately in these two physiological conditions. Finally, for the sake of simplicity, we investigate the plausible influence on outcomes of two, commonly used and transparent spatial filtering techniques, common average re-referencing (CAR) and Small Laplacian (SL) filtering, while also including raw (i.e., no spatial filter) EEG data as a control case. In summary, this simple experimental environment allows us to test if our conclusions regarding the change of E/I ratio in response to a trivial intervention would depend on our processing pipeline, evaluated in two cases: one where we expect an intervention effect, and another where we do not. To provide additional robustness to this notion, we carry out our analysis on two independent cohorts, in which EEG was collected with different electrode montages and reference schemes.

2 Materials and Methods

2.1 Participants and data collection

We analyzed EEG data collected in two separate studies, involving two independent, non-overlapping cohorts. Both projects were conducted in line with the regulations of the Declaration of Helsinki, and the protocols were reviewed and approved by the Institutional Review Board of The University of Texas at Austin (approval number: 2020-03-0073). All participants provided written informed consent before the measurement, and recordings were carried out in an isolated room with dim lighting, while participants were sitting in an armchair.

The first study cohort consisted of 24 young, healthy individuals (mean age 22.96 ± 2.63 years, 7 females, 22 right handed). EEG data was collected using an ANT neuro EEGO amplifier from 32 (international 10-10 standard) scalp locations, with the reference electrode positioned over CPz ('StimCap'). The electrode montage is illustrated on **Figure 1** (left). Note that channels FP1, FPz, FP2, T7, T8, M1 and M2 were excluded from analysis as these channels are more commonly affected by eye movements, blinks, and skeletal muscle artifacts, yielding 25-channel EEG data. Data

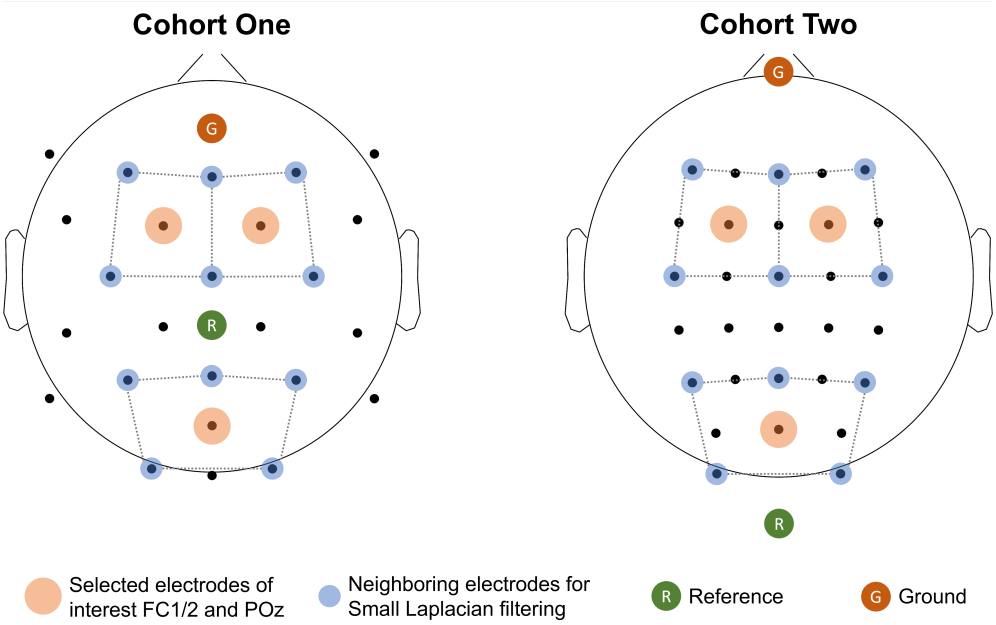

Fig. 1 Electrode montages utilized for data collection in Cohort One (left) and Cohort Two (right). Orange indicates electrodes of interest FC2 and POz. Blue indicates channels utilized for Small Laplacian filtering. Green and Red indicates the position of the reference (CPz for cohort on, Iz for cohort two) electrode and ground (AFz for cohort one, FPz for cohort two), respectively.

collection protocol involved one minute of EEG monitoring with eyes open followed by one minute with eyes closed, with a 10-second intermediary period in between.

The second study cohort consisted of 19 young, healthy volunteers (mean age 27.26 ± 6.11 years, 10 females, all right handed). In these recordings, EEG data was collected using a similar ANT neuro EEGO amplifier, however utilizing a customized cap that monitored neural activity from 32 of the international 10-5 standard locations ('ErrCap'). In this arrangement, electrode density was higher over the mid- and parasagittal lines, with the reference electrode positioned over the inion (Iz). Note that channels AF3 and AF4 were excluded from analysis due to their susceptibility to eye-related components, yielding 30-channel EEG data. The precise electrode layout is illustrated on **Figure 1** (right). Data collection protocol was similar to that of cohort one, only in these recordings two minutes of EO and EC data was collected instead of one.

In both cohorts, EEG data was sampled at 512 Hz, and all electrode impedances were kept under 5 kΩ. During both conditions participants were instructed to rest, not to engage in any specific mental activities, refrain from motion and stay awake. During EO recordings, a fixation cross was presented on a computer screen, on which participants were asked to focus their gaze on to minimize eye movements. In that, a total of three electrodes were positioned next to the canthi and above the left eye, with a common reference electrode positioned below the left eye.

2.2 Data pre-processing and selection

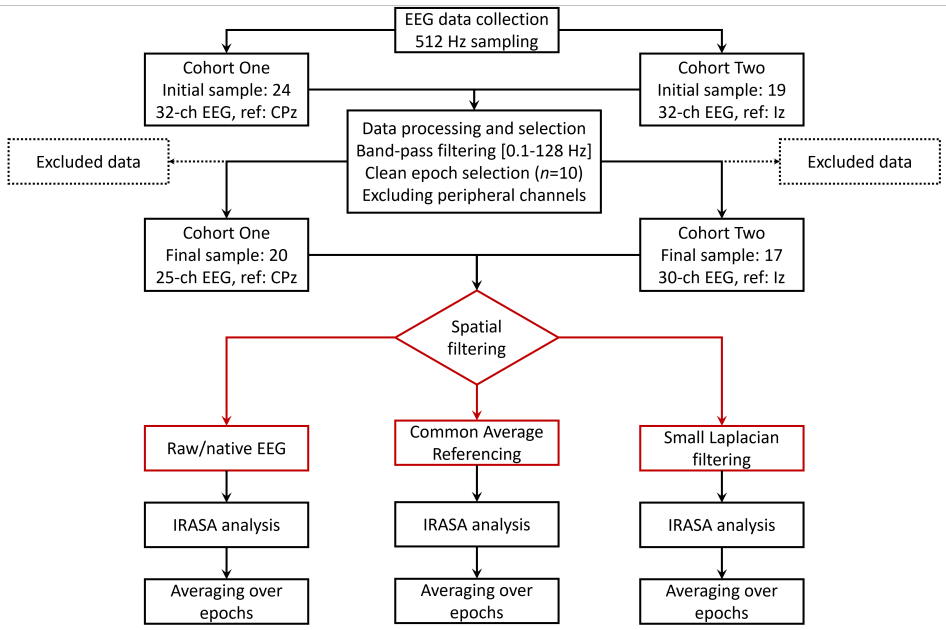

Fig. 2 Flowchart showing the different steps of the analysis pipeline. Spatial filtering step is highlighted in red to underscore the distinguishing step among the various protocols. EEG: electroencephalography; ch: channel; ref.: reference electrode position; IRASA: irregular-resampling auto-spectral analysis.

All data analyses, including pre-processing, obtaining of neural indices and statistics, were implemented and carried out in Matlab 2021b (The MathWorks, Nattick, USA). The data analysis pipeline is illustrated as a flowchart on **Figure 2**. Data was first visually inspected and datasets with one or more faulty channels or excessive noise were discarded. Raw data was band-pass filtered using a 4th-order, zero-phase Butterworth filter with cutoff frequencies 0.1 and 128 Hz. Then, segments containing absolute amplitude values above 100 μV in any of the EEG channels were excluded with additional padding of 1/16 s. Finally, segments with a length of 4 seconds were selected randomly from the remaining data, and those participants where this procedure could not yield at least 10 clean epochs in both conditions were also excluded from further analysis. This resulted in a final sample size of 20 and 18 participants in cohorts one and two, respectively. Finally, data epochs were subjected to one of the three spatial filtering schemes as detailed below.

As a representative frontal/prefrontal channel, we selected the FC2 location, while POz as a representative occipital/parietooccipital location. The reasoning for these picks stems from the electrode montage utilized in the two cohorts; namely, these were the most frontal and occipital available scalp locations for which we could apply SL filtering in the same exact manner (see below). To avoid potential bias from laterality,

analyses were carried out equivalently for FC1, too, however we only report those of FC2 in detail here.

Data was either re-referenced to the common average electrode (CAR scheme), subjected to small Laplacian filtering (SL scheme) or left untreated in the original reference arrangement (RAW scheme). During CAR, the average EEG signal computed over all channels and then subtracted from each individual channel FC2 and POz. In the SL scheme, average activity of neighbouring channels was computed and then subtracted from each respective channel [21]. For FC2 (and equivalently, FC1) these included locations Fz, F4 (F3), Cz and C4 (C3), while P3, Pz, P4, O1 and O2 for POz (see **Figure 1**).

2.3 Spectral slope analysis

Spectral slope estimates were obtained using the irregular resampling auto-spectral analysis (IRASA) technique introduced by Wen and Liu [4]. This method assumes a composite model where neural activity is treated as a superposition of scale-free/fractal and oscillatory/harmonic components. In this framework one can exploit the self-affine property of broadband scale-free signals [22], in that their power spectral characteristics are unaffected in distribution — and only subject to rescaling — by resampling, while this property does not hold for harmonic signals. Along these principles, one can devise a method to isolate the power spectra corresponding to the fractal component by taking the geometric mean of the power spectra obtained from up- and downsampled versions of the original signal [23, 24]. IRASA improves upon this principle by utilizing a set of non-integer resampling factors thus to reduce the probability of retained oscillatory peaks due to harmonic overlap [4]. After the scale-free spectrum is isolated, the spectral exponent (slope) can be estimated via OLS regression of log-transformed power over log-transformed frequency without the bias of present harmonic components such as alpha or theta peaks, or line noise and its harmonics at 60 and 120 Hz [4]. In addition, the isolated spectra of oscillatory components can also be obtained by subtracting the scale-free from the original power spectrum, assuming no phase coupling between scale-free and oscillatory components. For more details on the IRASA technique and its precise algorithm, please refer to [4] or [25].

In our analyses, IRASA was employed with the following parameter settings in the three processing pipelines (RAW, CAR and SL). Data was initially filtered in the 0.1-128 Hz range. The set of resampling factors was set to default from 1.1 to 1.9 in increments of 0.05, as recommended by Wen and Liu [4]. Spectral slopes were estimated from the fractal spectra in the 0.5-5 Hz (low-) and in the 20-60 Hz (high-) ranges. The boundary frequencies were set so the filtering effects introduced by resampling, as well as the documented 'smearing' of the spectra around the prominent alpha peak do not intersect with the ranges of interest (for more details see the Supplementary Material in [15]).

From each 4-second epoch, we obtained the spectral exponent for the low- (β_{lo}) and high- (β_{hi}) ranges. Additionally, to characterize inhibitory tone, we estimated log-transformed total and proportional oscillatory alpha power. In the former case, log-transformed total band-limited power was summed in the 8-12 Hz range (BLP^{α}_{total}). In the latter, first the proportion of oscillatory power was computed by subtracting

log-transformed scale-free spectrum from the log-transformed raw power spectrum, and then summed over the 8-12 Hz range (BLP^{α}_{osci}). To also explicitly measure the effect of closing the eyes, difference measures were obtained as $\Delta\beta_{lo} = \beta^{EC}_{lo} - \beta^{EO}_{lo}$ (and equivalently for β_{hi}) and $\Delta BLP^{\alpha}_{total} = BLP^{\alpha,EC}_{total} - BLP^{\alpha,EO}_{total}$ (and equivalently for $\Delta BLP^{\alpha}_{osci}$) where EO and EC in superscript denotes the physiological condition. Finally, for each participant, channel and condition, neural indices were averaged over the 10 epochs to obtain statistically robust estimates. Note that even though EEG spectral exponents are generally negative i.e., power decreases as frequency increases, conventionally we will refer to β_{lo} and β_{hi} as their absolute values [26] and thus e.g., a larger β_{hi} denotes a steeper high-range spectrum/slope and vice versa.

2.4 Statistical analyses

All variables were first tested for normality using the Kolmogorov-Smirnov test. Then, data was first evaluated via a 4-way repeated measures linear model with main effects frequency range (*range*, lo- vs. hi-range), physiological condition (*cond*, EO vs. EC), spatial filter ($filt$, raw vs. CAR vs. SL) and cortical location (*ch*, FC2 vs. POz). Beyond assessing if spectral exponents differ in low- and high-frequency regimes (*range*), if closing the eyes had an effect on spectral slope (*cond*), if spatial filtering affects slope estimates ($filt$) and if spectral slopes differ over various cortical locations (*ch*), all (2-, 3- and 4-way) interaction levels were also considered to evaluate if these conditions affect each other. Then, to emulate various study pipelines to address our core research question, we evaluated 6 cases for each channel-filtering scheme combination individually using 2-way repeated measures linear models with main effects *cond* and *range*. For all linear models, sphericity of the data was evaluated via Mauchly's test, and in case of violation main and interaction effect p-values were corrected using the Greenhouse-Geisser method. In case of a significant main effect or $cond \times range$ interaction, we performed post hoc pairwise comparisons using paired t-tests with Bonferroni correction. Pairwise comparisons were also performed for total and oscillatory alpha power between EO and EC states. In case of normally distributed data a paired t-test was used, while a Wilcoxon signed rank test otherwise. Outcomes were adjusted for multiple comparisons using the Bonferroni method. Finally, we also assessed if changes observed in spectral slopes are related to changes in inhibitory tone (i.e., resting alpha BLP). Since most difference indices did not satisfy the normality criterion, we characterized the plausible relationship between spectral ($\Delta\beta_{lo}$ and $\Delta\beta_{hi}$) and resting alpha power ($\Delta BLP^{\alpha}_{total}$ and $\Delta BLP^{\alpha}_{osci}$) difference indices using Spearman correlation. Outcomes were adjusted to multiple comparisons using the Bonferroni method.

3 Results

3.1 Cohort one

3.1.1 Power spectra and resting alpha power

Group-averaged power spectra are illustrated on **Fig.3** over FC2 (upper panels) and POz (lower panels). Left panels show spectra obtained from raw EEG data (i.e., no

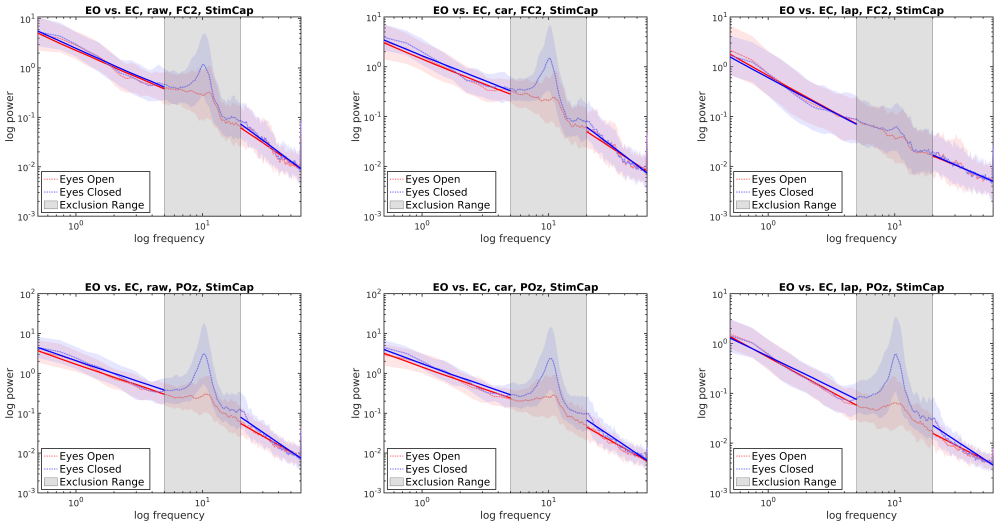

Fig. 3 EEG power spectra over FC2 (upper row) and POz (lower row) in eyes open (red) and eyes closed (blue) conditions. Columns from left to right show spectra obtained with no spatial filtering (raw), after common average re-referecing (car), and small Laplacian (lap) smoothing. The shaded gray area (from 5 to 20 Hz) indicate the range excluded from slope estimation, while straight lines show the fitted linear functions (obtained from isolated fractal spectra). Red and blue shaded areas indicate the standard error of the mean.

spatial filtering), while middle and right panels show the same for CAR- and SL-treated data, respectively. The panels show the native power spectrum (i.e., without separating scale-free and oscillatory components) in EO (red) and EC (blue) conditions, with the fitted power-law superpositioned. Note that these latter were obtained from isolated scale-free spectra. On most panels (with the exception of FC2 when using SL), a prominent alpha peak in EC is apparent at ~ 10 Hz, which is mostly absent in EO. Additionally, spectra of raw and CAR-treated data appear bimodal with steeper slope in the high- compared to the low-frequency range, while this bimodality is absent (or even reversed) for data subjected to SL filtering.

As a sanity check, we also verified if BLP^{α}_{total} and BLP^{α}_{osci} was higher in EC compared to EO states i.e., if our model physiological intervention had the hypothesized effect. The expected $BLP^{\alpha,EC}_{total} > BLP^{\alpha,EO}_{total}$ pattern was confirmed in all three spatial filtering schemes, over both FC2 and POz ($p < 10^{-4}$ for all cases except SL-data over FC2, where $p = 0.0331$). The equivalent results were obtained for BLP^{α}_{osci} in raw (FC2: $p < 0.0005$; POZ: $p < 10^{-4}$) and CAR cases ($p < 10^{-4}$ for both FC2 and POz), however in SL-treated data $BLP^{\alpha,EC}_{total} > BLP^{\alpha,EO}_{total}$ was only confirmed over POz ($p < 10^{-4}$) but not over FC2 ($p = 0.0951$).

3.1.2 Spectral slopes

Results of the 4-way model are presented in **Table 1**. We found a significant 4-way interaction of $filt \times ch \times cond \times range$ ($p = 0.0382$), indicating elaborate interplay between the investigated study aspects. Among 3-way effects, $filt \times ch \times range$ ($p = 0.0013$) and $ch \times cond \times range$ ($p = 0.0013$) indicated significant interaction. The

4-way repeated-measures linear model - Cohort one				
Main effects	SSE	DoF	F	p-value
$filt$	3.1805	38	51.467	$p < 10^{-7}$
ch	1.3872	19	6.0805	$p = 0.0234$
$cond$	1.5669	19	34.279	$p < 10^{-4}$
$range$	30.5872	19	22.619	$p = 0.0001$
2-way interaction effects	SSE	DoF	F	p-value
$filt \times ch$	0.2752	38	6.1505	$p = 0.0049$
$filt \times cond$	0.2256	38	4.6714	$p = 0.02435$
$ch \times cond$	0.1897	19	4.4792	$p = 0.04774$
$filt \times range$	18.627	38	217.38	$p < 10^{-13}$
$ch \times range$	1.9986	19	15.76	$p = 0.0008$
$cond \times range$	2.806	19	34.255	$p < 10^{-4}$
3-way interaction effects	SSE	DoF	F	p-value
$filt \times ch \times cond$	0.0297	38	0.8440	$p = 0.4333$
$filt \times ch \times range$	0.9507	38	10.153	$p = 0.0013$
$filt \times cond \times range$	0.0117	38	0.3833	$p = 0.6634$
$ch \times cond \times range$	0.4380	19	14.171	$p = 0.0013$
4-way interaction effect	SSE	DoF	F	p-value
$filt \times ch \times cond \times range$	0.1725	38	3.5809	$p = 0.0382$

Table 1 4-way repeated measures model to investigate the effect and interaction between spatial filtering, frequency range, physiological state and cortical location. SSE: sum of squared errors; DoF: degrees of freedom; F: F-statistic; $filt$: spatial filtering scheme; ch: channel/cortical location; $cond$: physiological condition; $range$: frequency regime.

former suggests that spatial filtering does affect how β_{lo} and β_{hi} is different over prefrontal and occipital brain regions, while the latter implies that this difference is also responsive to change in physiological state. Notably, all 2-way interaction effects indicated significant interplay between the main effects. Finally, all four main effects were significant, confirming that all investigated factors have substantial effect on the spectral exponent.

Our core research question was if applying different spatial filtering schemes, can we arrive at different conclusions in terms of how spectral slope (and thus inferred E/I ratio) is affected by changing the physiological state. For clear presentation, we investigated this for the three spatial filtering schemes over the two cortical locations independently with 2-way repeated measures models; results of these analyses are presented on **Figure 4**. Over Fc2, a significant $state \times range$ interaction effect was found in raw ($p = 0.0040$) and CAR-treated ($p = 0.0006$), but not for SL-treated ($p = 0.1576$) data, indicating that the effect of closing the eyes is different in low- and high-regimes in the first two cases, but not the third. Post hoc tests confirmed that while β_{lo} was smaller (i.e., the spectrum was less steep) compared to β_{hi} in both EO

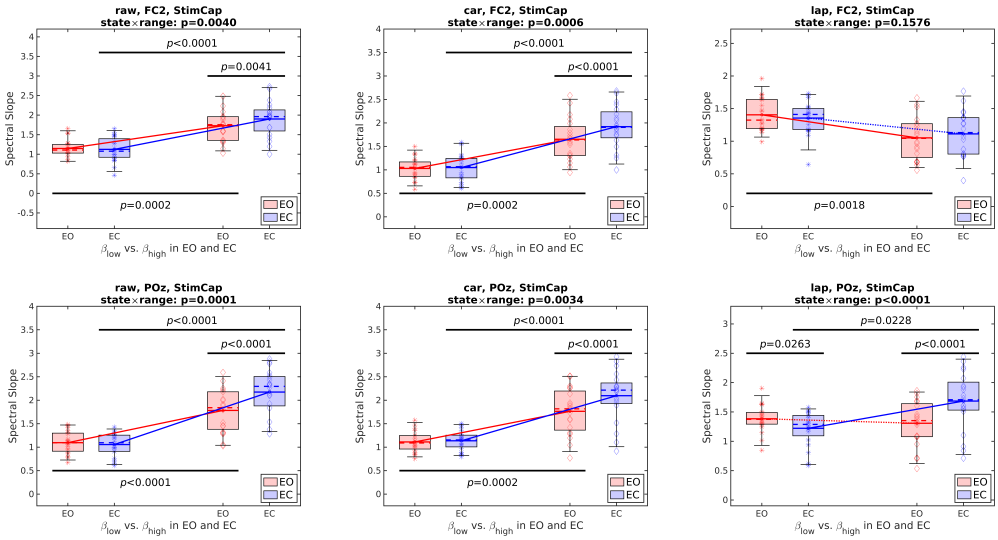

Fig. 4 Spectral slope estimates from low- (β_{lo}) and high- (β_{hi}) frequency regimes in Cohort one. Upper and lower rows present box plots from FC2 and POz regions and red and blue colors indicate eyes open and eyes closed states, respectively. On each panel, box plots on the left and right illustrate low- and high-range β values in the two conditions, respectively. Horizontal black bars indicate significant pair-wise difference (p<0.05, adjusted) between corresponding cases.

and EC, however closing the eyes only increased β_{hi} significantly, but not β_{lo}. On the other hand, a substantial $filter \times range$ interaction ($p < 10^{-13}$) indicated that spatial filtering affects this $\beta_{lo} < \beta_{hi}$ relationship (**Table 1**). In line, post hoc comparisons on SL-treated data indicated that β_{lo} is significantly higher than β_{hi} in EC; in other words, the bimodal nature of EEG spectra reversed due to SL filtering. Furthermore, there was no longer a significant increase in β_{hi} due to closing the eyes.

We found comparable results over POz. Namely, the EEG spectrum was bimodal with β_{lo} being significantly lower than β_{hi} in both EO and EC conditions for raw and CAR-treated data, while closing the eyes resulted in an increase in β_{hi} compared to EO. Results for SL-treated data, however, were different: the $state \times range$ interaction was significant ($p < 0.0001$). Post hoc comparisons not only indicated, that $\beta_{lo} < \beta_{hi}$ in EC (i.e., the nature of bimodality is unaltered in EC), but also while closing the eyes further reduced β_{lo}, in resulted in an increase of β_{hi}.

In summary, these outcomes have two very important implications. First and foremost, outcomes obtained over FC2 explicitly show that one can arrive to different conclusions by CAR and SL spatial filtering: while the former indicates an decrease in E/I ratio as captured in physiological state related increase in β_{hi}, this effect is absent in the latter case. Second, results over POz when pre-processed using SL filtering support the notion that β_{lo} and β_{hi} likely express an opposite relationship with E/I ratio, in line with previous findings [9, 16].

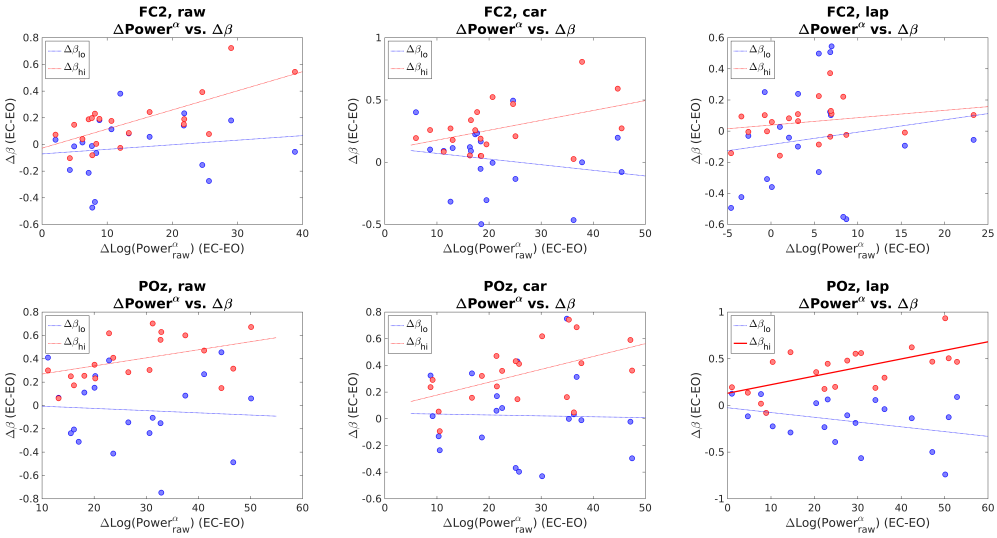

Fig. 5 Correlation between the change in resting total alpha power and the change in spectral slopes in Cohort one. Top and bottom row panels illustrate the outcomes for FC2 and POz, respectively in all three pre-processing schemes (from left to right: raw, CAR-referenced and Laplacian-smoothed data). Blue and red samples denote estimates for low- (β_{lo}) and high- (β_{hi}) range spectral slopes. Straight lines show the ordinary least squares regression line fitted on the datasets in matching colors; a continuous straight line indicates statistically significant correlation ($p < 0.05$, adjusted) between the two variables (in contrast to dotted lines).

3.1.3 Correlation between spectral slope and resting alpha power

Finally, to provide support that the observed changes in β are related to a change in inhibitory tone, we made an attempt to characterize their plausible relationship. (**Figure 5**) illustrates the relationship between slope difference indices $\Delta\beta_{lo}$ and $\Delta\beta_{hi}$, and $\Delta BLP^{\alpha}_{total}$. After multiple comparisons adjustment, we only observed a significant positive correlation between $\Delta\beta_{hi}$ and $\Delta BLP^{\alpha}_{total}$ ($r = 0.6259, p = 0.0.379$) over POz for SL-treated data, indicating that a stronger increase in resting alpha power due to closing the eyes was associated with the high-frequency spectrum becoming steeper. Although this pattern appears to be in line with our previous results and the slope-E/I ratio hypothesis, we could only confirm this relationship for total alpha power — including both broadband 'background activity' and harmonic alpha oscillations — but not for isolated oscillatory alpha power, and therefore these results should be interpreted with caution. Notably, no relationship was found at all between $\Delta\beta_{lo}$ and resting alpha power.

3.2 Cohort two

Although results obtained from Cohort one already provided an answer to our initial research question, we wanted to investigate this phenomenon robustly, also confirming that the observed effects are not a peculiarity of the given EEG electrode montage and reference scheme. To this end, we carried out our analysis pipeline on an independent dataset, where EEG was collected using a different electrode montage (see **Figure 1**).

In summary, outcomes of the analysis of Cohort two confirmed those of Cohort one, as detailed below.

3.2.1 Power spectra

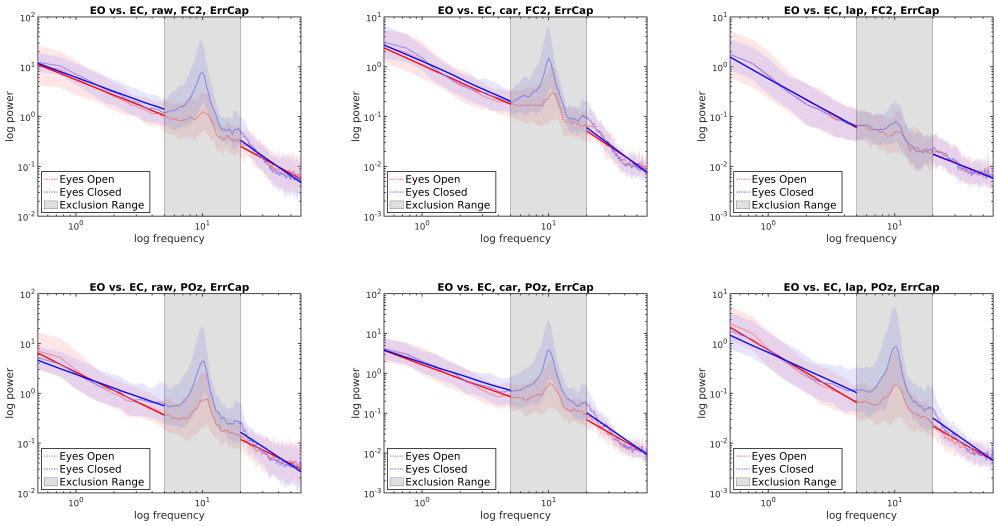

Fig. 6 EEG power spectra over FC2 (upper row) and POz (lower row) in eyes open (red) and eyes closed (blue) conditions. Columns from left to right show spectra obtained with no spatial filtering (raw), after common average re-referecing (car) and small Laplacian smoothing (lap). The shaded gray area (from 5 to 20 Hz) indicate the range excluded from slope estimation, while straight lines show the fitted linear functions (obtained from isolated fractal spectra). Red and blue shaded areas indicate the standard error of the mean.

Group-averaged power spectra from Cohort two are illustrated on **Fig.6** over FC2 (upper panels) and POz (lower panels). The same patterns are observed as on **Fig.3**, only the inversion of the $\beta_{lo} < \beta_{hi}$ bimodality pattern over FC2 in SL-treated data is even more apparent.

When investigating BLP^{α}_{total} and BLP^{α}_{osci} in EC and EO states, outcomes were almost identical as in Cohort one. BLP^{α}_{total} was higher in EC compared to EO in all three spatial filtering pipelines, over both FC2 and POz ($p < 0.0089$ in all cases). On the other hand, $BLP^{\alpha,EC}_{osci} > BLP^{\alpha,EO}_{osci}$ was only statistically significant for raw and CAR-treated data over both scalp locations ($p < 0.0205$ in all cases), while the same difference was only tendential in SL-treated data (FC2: $p = 0.0869$; POz: $p = 0.0574$).

3.2.2 Spectral slopes

Results of the 4-way model evaluated on Cohort two are presented in **Table 2**. Overall, the outcomes are comparable with those presented in **Table 1**, with some important distinctions. The 4-way interaction again indicated a significant interplay between the main model effects ($p = 0.0059$). Main effects $filt$, ch and $range$ indicated significant influence of spatial filtering ($p = 0.0022$), cortical location ($p = 0.0061$) and

4-way repeated-measures linear model - Cohort two				
Main effects	SSE	DoF	F	p-value
$filt$	4.408	34	11.385	$p = 0.0022$
ch	1.2928	17	9.8162	$p = 0.0061$
$cond$	0.4401	17	2.6945	$p = 0.1191$
$range$	17.928	17	15.426	$p = 0.0011$
2-way interaction effects	SSE	DoF	F	p-value
$filt \times ch$	1.4806	34	25.892	$p < 10^{-6}$
$filt \times cond$	0.1441	34	2.0376	$p = 0.1631$
$ch \times cond$	0.0446	17	1.6324	$p = 0.2185$
$filt \times range$	13.846	34	35.77	$p < 10^{-6}$
$ch \times range$	1.3627	17	6.9605	$p = 0.0173$
$cond \times range$	5.7625	17	44.255	$p < 10^{-5}$
3-way interaction effects	SSE	DoF	F	p-value
$filt \times ch \times cond$	0.0880	34	2.9215	$p = 0.0778$
$filt \times ch \times range$	4.3189	34	43.28	$p < 10^{-7}$
$filt \times cond \times range$	0.4111	34	7.891	$p = 0.0026$
$ch \times cond \times range$	1.0315	17	26.823	$p < 10^{-4}$
4-way interaction effect	SSE	DoF	F	p-value
$filt \times ch \times cond \times range$	0.1847	34	6.8435	$p = 0.0059$

Table 2 4-way repeated measures model to investigate the effect and interaction between spatial filtering, frequency range, physiological state and cortical location. SSE: sum of squared errors; DoF: degrees of freedom; F: F-statistic; $filt$: spatial filtering scheme; ch: channel/cortical location; $cond$: physiological condition; $range$: frequency regime.

spectral bimodality ($p = 0.0011$). Interestingly, *cond* turned out to be non-significant ($p = 0.1191$), suggesting that closing the eyes had no consistent effect on spectral slopes. On the other hand, the interaction of $cond \times range$ indicated a strong effect ($p < 10^{-5}$), possibly denoting that β_{lo} and β_{hi} might change in opposite directions in response to the physiological intervention. Furthermore, the 3-way interaction $filt \times cond \times range$ implied that this effect is significantly modulated by the choice of spatial filtering scheme ($p = 0.0026$). The $filt \times ch$ interaction strongly implied that spatial filtering affects slope estimates over FC2 and POz differently, and the $filt \times ch \times range$ interaction revealed that this effect is likely unique for low- and high-range estimates.

When investigating β_{lo} and β_{hi} estimates in separate 2-way models **Figure 7**, we found almost identical results over FC2 to those presented on **Figure 4**. Precisely, $cond \times range$ interaction was significant for raw ($p < 10^{-4}$) and CAR-treated ($p = 0.0044$) data but not for SL filtering ($p = 0.4744$). Post hoc comparisons indicated significant spectrum bimodality with $\beta_{lo} < \beta_{hi}$ in EC for raw and CAR-treated data ($p < 10^{-4}$ both) and also for EO in the latter case ($p = 0.0024$). On the other

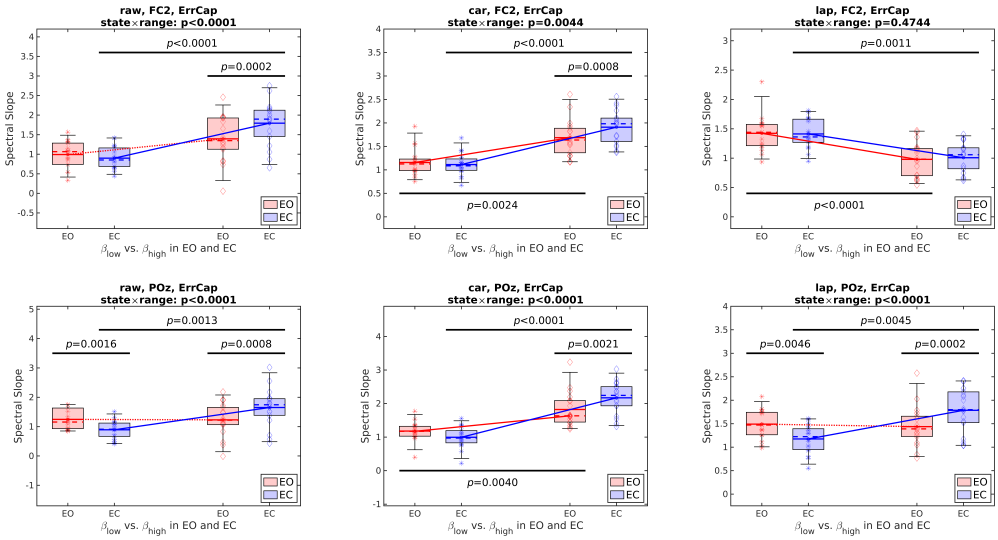

Fig. 7 Spectral slope estimates from low- (β_{lo}) and high- (β_{hi}) frequency regimes in Cohort two. Upper and lower rows present box plots from FC2 and POz regions and red and blue colors indicate eyes open and eyes closed states, respectively. On each panel, box plots on the left and right illustrate low- and high-range β values in the two conditions, respectively. Horizontal black bars indicate significant pair-wise difference (p<0.05, adjusted) between corresponding cases.

hand, while *range* had a significant main effect in the SL pipeline ($p < 10^{-4}$), post hoc tests revealed that the bimodality pattern again was reversed with $\beta_{lo} > \beta_{hi}$ for both EO ($p < 10^{-4}$) and EC ($p = 0.0011$). Perhaps even more importantly, while pairwise comparisons confirmed an increase of β_{hi} in response to closing the eyes in raw ($p = 0.0002$) and CAR-treated EEG ($p = 0.0008$), this effect was absent in the SL filtering pipeline. Therefore, these outcomes again confirmed that while one would conclude that closing the eyes increased inhibitory tone/reduced the E/I ratio over FC2 when the data was unfiltered or CAR filtering was applied, the same analysis on SL-filtered data would instead indicate that closing the eyes had no significant effect on the E/I ratio.

Similarly, results from POz were almost identical to those obtained from Cohort one. Namely, the *cond* × *range* interaction was significant in all three pre-processing pipelines ($p < 10^{-4}$ in all cases), and while an increase of β_{hi} in response to closing the eyes were confirmed in all pipelines ($p = 0.0008$, $p = 0.0021$ and $p = 0.0002$ for raw, CAR- and SL-treated data, respectively), in the raw ($p = 0.0016$) and SL ($p = 0.0046$) pipelines it was also revealed that going from EO to EC results in a decrease of β_{lo}. Finally, the $\beta_{lo} < \beta_{hi}$ bimodality patterns was consistent for all three cases for EC ($p = 0.0013$, $p < 10^{-4}$ and $p = 0.0045$ for raw, CAR and SL, respectively), and while the same pattern was only observed in CAR-treated data in EO ($p = 0.0040$), in none of the remaining cases we saw an inversion where β_{lo} becomes larger than β_{hi}. Therefore, these results also provide further support that an increase in inhibitory tone — that we can expect over the occipital cortex when transitioning from EO to EC — result in a simultaneous increase and decrease of β_{hi} and β_{lo}, respectively.

3.2.3 Correlation between spectral slope and resting alpha power

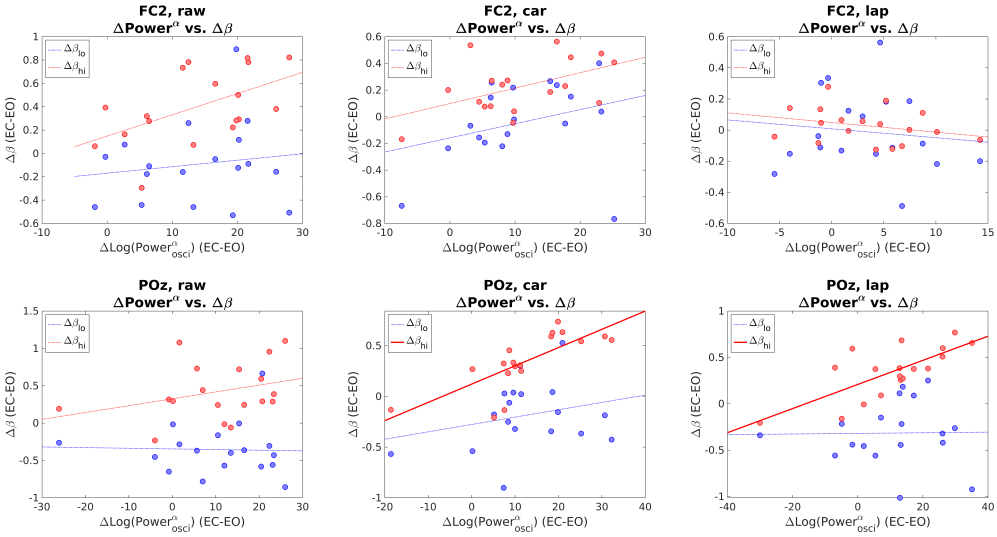

Fig. 8 Correlation between the change in resting oscillatory alpha power and the change in spectral slopes in Cohort two. Top and bottom row panels illustrate the outcomes for FC2 and POz, respectively in all four pre-processing schemes (from left to right: raw, CAR-referenced, and Laplacian-smoothed data). Blue and red samples denote estimates for low- (β_{lo}) and high- (β_{hi}) range spectral slopes. Straight lines show the ordinary least squares regression line fitted on the datasets in matching colors; a continuous straight line indicates statistically significant correlation ($p < 0.05$, adjusted) between the two variables (in contrast to dotted lines).

Nevertheless, to further confirm that changes in β are indeed related to inhibitory tone, we evaluated the relationship between spectral slope change and alpha power change in response to closing the eyes. Notably, a significant positive correlation between $\Delta\beta_{hi}$ and $\Delta BLP^{\alpha}_{total}$ (data not shown) was revealed over FC2 for CAR-filtering ($r = 0.6737, p = 0.0261$), while the same pattern was observed over POz for CAR ($r = 0.8434, p = 0.0001$) and SL ($r = 0.7979, p = 0.0008$). Furthermore, when changes in slope were contrasted with changes in isolated oscillatory alpha power (**Figure 8**), this positive correlation was still significant over POz for the CAR ($r = 7569, p = 0.0033$) and SL ($r = 0.7271, p = 0.0075$) cases. These outcomes now provide more sound support to the notion that the increase observed in β_{hi} over POz was due to an increase in inhibitory tone and thus a reduction in the E/I ratio, but it also must be noted that we did not observe a negative correlation between $\Delta BLP^{\alpha}_{osci}$ and $\Delta\beta_{lo}$.

4 Discussion

In this study we carried out a systematic evaluation to confirm if different EEG pre-processing pipelines and analytical settings can substantially affect estimates of the

spectral slope, with a special focus on the question if these effects can lead to contradictory inferences regarding cortical E/I ratio. Our results clearly demonstrate that analyzing EEG data with varying protocols can indeed yield conflicting conclusions even within a confined, comparative experimental environment. Moreover, our complementary analysis of a second, independent dataset with dissimilar data collection specifics produced nearly identical outcomes, further highlighting the importance and general nature of our central research question. The results presented here therefore warrant the establishing of a standardized data analysis pipeline for studies aiming at drawing inferences on cortical E/I ratio from EEG data.

4.1 Insights on the relationship between spectral slope and E/I ratio

Although previous literature has established that the power spectrum of electrophysiological recordings of brain activity express multiple scaling ranges with significantly different scaling exponents [6, 14, 15, 27], this notion was so far often neglected in recent studies probing the E/I ratio via the spectral slope. Some studies [11] limited their range for estimating β roughly to the 30-50 Hz following the original model of Gao and colleagues [7], while in other cases only lower-range analysis was applicable due to technical limitations [28]. However, in multiple cases the considered frequency regime spanned approximately 2-25 Hz [29–31] or a broadband 1-45 Hz [10, 12, 13], while not many articles reported analysis outcomes treating low- and high-range slopes separately [9, 15]. In this study we provide further support for the notion that low- and high-range spectral exponents should be analyzed individually. The previously reported observation of $\beta_{lo} < \beta_{hi}$ [6, 14] was most apparent for raw and CAR-referenced data (see **Figures 4** and **7**); however, SL spatial filtering could eliminate, or even revert this pattern, especially over FC2 (in line with [15]). Importantly, none of the aforementioned studies utilized exactly the same data processing pipeline; CAR appeared as the most frequently utilized spatial filtering technique [9, 12, 28], while other studies implemented re-referencing to mastoids [30] or earlobes [31]. Additionally, many studies employed more elaborate manipulations to the data such as independent component analysis (ICA)-based artifact removal [9–11, 28, 30], that could introduce further effects that we did not investigate in this work. While these factors prevent a fair and objective comparison of outcomes from these independent studies — and by no means undermine their contribution to the scientific literature —, given our results here we argue that spectral slope estimation should be implemented separately for low- and high-frequency regimes, not solely based on the fact that β_{lo} and β_{hi} estimates can be statistically significantly different, but because they apparently respond to change in physiological state in varying ways [9]. For the datasets analyzed here, this was most apparent for SL-fitlered data over POz, where closing the eyes resulted in a decrease in β_{lo}, and a simultaneous increase in β_{hi} (**Figures 4** and **7**). Finally, we evaluated results when assessing the spectral slope unimodally from a broadband 0.5-45 Hz range (β_{bb}), similar to previous studies [10, 12, 13]. In cohort One, we only observed a difference in β_{bb} with response to closing the eyes in one case: β_{bb} in EC was lower (1.1730 ± 0.1670) over POz compared to

in EO (1.2189 ± 0.1982) for SL-processed data (paired t-test, $p = 0.0023$, Bonferroni-adjusted). In Cohort Two, the same difference was observed over POz for all three pre-processing techniques ($p < 0.0260$ in all cases, Bonferroni-adjusted), but still no physiological state-related difference was observed over FC1 or FC2. The nature of this difference indicates that i) β_{bb} reflect similar effects as β_{lo}, and ii) the preprocessing scheme can still influence the study outcomes, as demonstrated in Cohort One. Interestingly, while state-related changes in β_{bb} was never found correlated with ΔBLP^{α}, in Cohort Two we found a negative correlation between the two variables in SL-treated EEG data over POz (Spearman $r = -0.6755$, $p = 0.0251$). This would be in contradiction with original notion put forward by Gao and colleagues [7] by suggesting that a supposed increase in inhibitory tone (going from EO to EC) actually reduces the spectral slope, while if β_{bb} estimates are primarily driven by those of β_{lo}, then it is in line with the results of Becker and coworkers [16]. While this question may warrant further investigations, overall, given our results we strongly support that the spectral slope should be characterized independently for low- and high-frequency regimes.

We followed the same assumption as Becker and colleagues [16] in that resting alpha power is a correlate of inhibitory tone [17]. Consequently, we could also hypothesize that closing the eyes will produce a stronger increase in inhibition over occipital compared to frontal brain areas [19]. Indeed, in most cases we could confirm that the increase in alpha power in response to closing the eyes was significantly smaller over the FC2 compared to POZ region (data not shown). In this framework, our results suggest that SL filtering might be superior to CAR or keeping the native reference scheme with regards to drawing inferences on the E/I ratio. Precisely, according to the original model in [7], from raw and CAR-treated data one would conclude that the E/I ratio decreased due to closing the eyes over both FC2 and POz, as indicated by an increase in β_{hi}. On the other hand, when EEG data was spatially filtered with SL, one would only came to this conclusion with regards to POz but not FC2. This is also supported by correlation analysis between $\Delta\beta_{hi}$ and ΔBLP^{α} that consistently showed a positive relationship over POz on SL-filtered data (see **Figures 5** and **8**). Furthermore, only with SL spatial filtering could we observe a simultaneous decrease in β_{lo} when transitioning from EO to EC, as one could expect from the results of Becker et al. [16] and Muthukumaraswamy & Liley [9]. Note that to eliminate the potential bias of laterality, we carried out our complete analysis pipeline with selecting POz and FC1 instead of FC2, leading to equivalent outcomes and conclusions in both study cohorts. While our observations appear crucial, they are also somewhat expected and understandable based on the characteristics of CAR and SL. While the goal of SL spatial filtering is to localize brain activity and improve spatial resolution, CAR filtering is efficient in removing global signal components, while at the same time distributing neural activity (to some extent) over all channels [32]. In alignment with our assumptions over the effects of closing the eyes as well as the expected topology of inhibitory tone, this explains why SL was the pre-processing scheme producing the expected results, while a plausible explanation of the outcomes observed for CAR is that it resulted in some of the activity from occipital regions to be carried over to prefrontal channels. Interestingly, outcomes from raw EEG and CAR were strongly aligned, especially in Cohort

One. On the other hand, in Cohort Two, spectral bimodality in EO was only apparent after CAR filtering, over both prefrontal and occipital regions (**Figure 7**). This points to the initial role of the reference position: In Cohort One — where bimodality was ubiquitously present even in raw EEG data (**Figure 4**) —, the reference (CPz) was approximately the same distance from the two regions of interest, while in Cohort Two (over Iz) it was in close proximnity to POz but not to FC2/FC1 (see also **Figure 1**). It is well established that the reference position can have significant influence on EEG signal power [33] or estimated brain network structure [34], but less is known about its potential confounding effects on the spectral slope [35]. Although we did not explore this aspect any further here, this appears as an interesting question that we intend to pursue in the future. Nevertheless, we tentatively draw two overall conclusions from these ramifications: foremost, it is robustly confirmed that CAR and SL filtering would lead us to conflicting inferences on the change of E/I ratio in response to closing the eyes, as well as SL — and other spatial filtering techniques promoting localization of neural activity, such as current source density (CSD) transformation [36] — appears as the suitable choice for data processing when one sets out to analyze the spectral exponent of EEG data.

4.2 Why spatial filtering affects spectral slope estimates?

The results presented here empirically highlight the seminal importance of the selection of spatial filtering technique in EEG spectral slope analysis; however, they do not allow insight on the origins of the observed phenomena. While we believe that a systematic investigation of this question is beyond the scope of this study, below we make an attempt to address this question from an intuitive angle.

While CAR and SL serve different purposes and therefore both have their preferred use cases, they share a common feature: both involve the summation (averaging) of multiple EEG time series, that are then subtracted from the channels of interest. Note that this latter step is also involved in standard re-referencing to a selected location. We believe that the key aspect to consider here is that this manipulation does not simply involve addition of two (or more) stochastic, independent time series but instead those with a $1/f$ spectra. It has been widely recognized that the superposition of two $1/f^{\beta}$ processes with different spectral exponents β_1 and β_2 can introduce a crossover in the power spectrum — or equivalently, the scaling function in the time domain — of the composite time series [27, 37–39]. Given the superposition of two theoretical processes with infinite length and sampling and with $\beta_1 > \beta_2$, the variance profile of process 2 (i.e., where the spectral power decays at a slower rate with increasing frequency) will eventually dominate that of process 1 as frequency increases, resulting in a power spectrum with a steeper slope (dominated by β_1) for lower frequencies and a slope close to β_2 for high frequencies, and a transition zone in between [38, 40]. An illustration of such a case is presented on **Figure 9A**. Note that the appearance of such a crossover will also depend on the total variance of the processes, as well as the frequency resolution/sampling. Theoretically, this argument holds for the superposition of an arbitrary number of time series (for an example, see **Figure 9B**), though it is worth highlighting that the estimation error with respect to the theoretical value of the spectral exponent increases with the number of superposed signals. Notably, this

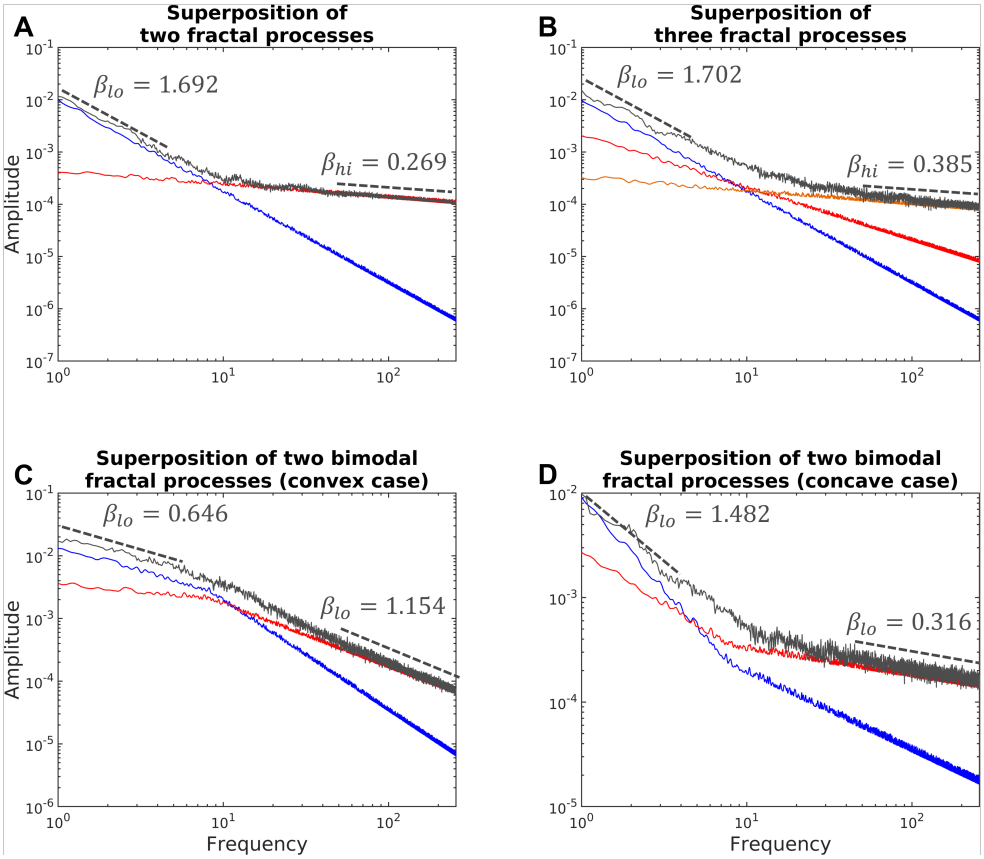

Fig. 9 Illustration of how the superposition of multiple $1/f$ signals can result in a crossover in the power spectrum. Spectra of composite time series are always denoted in dark gray. A: superposition of two $1/f$ signals with theoretical $\beta = 1.75$ (blue) and $\beta = 0.25$ (red). The power spectrum of the composite time series is apparently dominated by the larger exponent in the low-, while by the smaller exponent in the high-frequency regime. B: superposition of three $1/f$ signals with theoretical $\beta = 1.75$ (blue), $\beta = 1$ (red) and $\beta = 0.25$ (orange). In the low-frequency range, the spectral slope is dominated by the largest exponent, while by the smallest in the high-frequency regime. C: superposition of two bimodal signals where $\beta_{lo} < \beta_{hi}$; for the blue signal, β_{lo} and β_{hi} was set to 0.75 and 1.75, respectively, while for the red signal $\beta_{lo} = 0.25$ and $\beta_{hi} = 1$. Apparently, the low-frequency range is dominated by the blue signal with larger exponent in the given range, while the opposite holds for high-frequency range. D: superposition of two bimodal signals where $\beta_{lo} > \beta_{hi}$; for the blue signal, β_{lo} and β_{hi} was set to 1.75 and 0.75, respectively, while for the red signal $\beta_{lo} = 1$ and $\beta_{hi} = 0.25$. The previous observations regarding the dominant spectral exponent still hold. $1/f$ time series were generated by, and slope estimates were obtained via the IRASA toolbox [4].

phenomenon applies similarly to processes with known bimodal spectra, regardless if $\beta_{lo} < \beta_{hi}$ (**Figure 9C**) or $\beta_{lo} > \beta_{hi}$ (**Figure 9D**). From these considerations comes straightforward how data manipulations involving the summation and/or subtraction of multiple EEG signals can have a substantial effect on the spectral slope.

Nevertheless, the aforementioned argument only provides intuitive support but not a sound explanation. Most importantly, this notion only holds as is for time series

that are independent, which is clearly untrue for EEG channels, as supported not only by the vast literature on EEG-derived functional connectivity studies [41], but also self-evident from the volume conduction effects inherent to EEG methodology [42]. Furthermore, to capture and formally express the effects of more elaborate manipulations to data such as CSD transformation or ICA-based noise removal on the power spectral slope is far from trivial. For this reason, in this confined study we intentionally selected a single common step in EEG analysis and limited our exploration to techniques that are easily understandable (namely, CAR and SL). Nevertheless, this question is seminal for the derivation of a standardized data processing pipeline with a sound theoretical foundation and warrants further research; which is our central goal in the future.

4.3 Limitations and future work

The most important limitation of this work comes from the experimental design: while the observed outcomes empirically support the claim that various data processing steps can affect study conclusions, in terms of interpretation we can still only rely on suppositions in contrast to explicit neuroscientific evidence. Namely, we made two key assumptions based on previous literature: first, we took resting alpha power as a proxy for inhibitory tone [20] and thus EC resting as a state of increased inhibition (reduced E/I ratio) in contrast to EO [16, 17], and second, we hypothesized that this response in inhibitory tone will be more prominent over occipital compared to prefrontal regions [19]. Therefore, while the outcomes most consistently observed for SL-treated data are aligned with these initial assumptions, we cannot contrast them with 'ground truth' measurements of cortical E/I ratio or inhibitory tone in the investigated locations. Although we believe that this does not reduce the technical relevance of the results presented here, it definitely emphasizes the need for more elaborate investigation where the E/I ratio is explicitly and selectively controlled with some appropriate neuromodulation technique such as transcranial electrical [43] or magnetic [44] stimulation. Therefore, it is amidst our immediate goals to replicate our results in such an environment, where we have explicit control and monitoring options of the cortical E/I ratio, and thus we can truly interpret our findings in terms of neurobiology and take further steps towards suggesting an optimal pre-processing pipeline for EEG-based E/I analyses.

Another rightful question can be raised regarding our choice of the evaluation technique, IRASA [4]. IRASA was published in 2016 — building on concepts first introduced in 1991 [23] —, however another popular method termed 'fitting fitting oscillations & one over f' (FOOOF) was introduced recently (in 2020) to separately characterize the broadband $1/f$ and superimposed oscillatory components of neurophysiological signals [8]. FOOOF gained immense popularity in the past years and likely is the most frequently used technique for similar analyses (see e.g., [10–13, 31]). FOOOF arguably has advantages over IRASA in terms of allowing for a broader range for parametrization of oscillatory components, while the latter puts the emphasis on the unbiased estimation of the spectral slope via OLS regression. Another core difference is the approach for separating the $1/f$ component: FOOOF implements a data driven, recursive approach, while IRASA is a model-based technique, assuming an

additive signal model and exploiting the theoretical self-affinity property of the presumed fractal signal component. Overall, both methods can have favorable properties in a given situation [8], yet we decided to implement our analysis pipeline employing IRASA for one main reason. It has been observed previously that human neurophysiological recordings can indeed express power spectra where $\beta_{lo} > \beta_{hi}$ [27, 45, 46]. A key detail is that instead of a simple power-law function, FOOOF models the aperiodic component as a Lorentzian function with a 'knee' parameter [8]. This model inherently allows for the characterization of the slope only in the high-frequency range (i.e., after the 'knee') and thus is unsuitable for treating signals where $\beta_{lo} > \beta_{hi}$. Nevertheless, as a sanity check we executed our analysis pipeline using FOOOF focusing only on the high-frequency regime and obtained comparable outcomes with those using IRASA (data not shown). In the future, a combination of IRASA and FOOOF appears reasonable to take advantage of both methods, e.g., to use IRASA to characterize the $1/f$ spectra in low- and high-frequency regimes separately regardless of the nature of bimodality, while utilizing FOOOF to parametrize oscillatory peaks.

Besides these notions, we can identify other aspects where we can extend our work in the future. To some extent our analyses were constrained by technical details, as we had to select POz and FC2 (FC1) as regions of interest due to the available electrode montages (see **Figure 1**). Higher spatial resolution EEG would allow us to more specifically select brain regions suitable for a given employed intervention paradigm. Also, we did not employ a personalized approach for assessing alpha activity around the individual peak frequency [47] but instead characterized alpha power universally in the 8-12 Hz range. FOOOF could indeed enhance this aspect for our investigation by parametrizing alpha peaks — and thus help fine tuning low- and high scaling ranges, too — for each participant individually [8]. The relationship between the change in spectral exponents and resting alpha power was only assessed via correlation analysis due to the characteristics of the data, however this does not necessarily proof causality i.e., that a change in E/I ratio was the reason for the change in the spectral slope. Furthermore, this relationship was only significant for β_{hi} but not β_{lo} in any of the cases, which calls for more caution when linking β_{lo} to E/I ratio despite previous reports [9, 16]. Finally, our analysis here was limited to EEG, though same considerations should be made for analyzing the $1/f$ properties of neural activity recorded with other modalities such as magnetoencephalography [11, 48].

5 Conclusions

To summarize, in this study we provided empirical evidence that the choice of preprocessing pipeline can lead to conflicting interpretations of the outcomes even in an isolated, comparative experimental environment. We confirmed this notion robustly on two independent datasets, while also pointing out limitations and potential directions for future research. Overall, our results suggest that a spatial filtering step that aims on improving spatial resolution and localization of neural activity is preferred when estimating the spectral slope. Given the growing interest surrounding cortical E/I ratio and how it might be affected in various physiological and pathological conditions, our

results call for the establishing of a standardized evaluation protocol, so to render studies with similar interest as confluent and comparable as possible.

6 Author contributions

FSR conceptualized the project, contributed to data collection, performed data analysis and wrote the initial draft of the manuscript. DMA contributed to data collection. FSR, PM, JM, JLC and JdRM contributed to results interpretation and discussion. All authors contributed to the preparation of the manuscript, reviewed the draft and gave approved to its final version.

7 Acknowledgments

This study was funded in part by the Charley Sinclair Foundation and the Coleman Fung Foundation.

8 Conflict of Interest

None of the authors declare any financial or other conflicts of interest regarding this work.

9 References

References

[1] He, B. J. Scale-free brain activity: past, present, and future. *Trends in cognitive sciences* **18**, 480–487 (2014).

[2] Grosu, G. F. *et al.* The fractal brain: scale-invariance in structure and dynamics. *Cerebral Cortex* **33**, 4574–4605 (2023).

[3] Eke, A. *et al.* Physiological time series: distinguishing fractal noises from motions. *Pflügers Archiv* **439**, 403–415 (2000).

[4] Wen, H. & Liu, Z. Separating fractal and oscillatory components in the power spectrum of neurophysiological signal. *Brain topography* **29**, 13–26 (2016).

[5] Buzsaki, G. & Draguhn, A. Neuronal oscillations in cortical networks. *science* **304**, 1926–1929 (2004).

[6] Miller, K. J., Sorensen, L. B., Ojemann, J. G. & Den Nijs, M. Power-law scaling in the brain surface electric potential. *PLoS computational biology* **5**, e1000609 (2009).

[7] Gao, R., Peterson, E. J. & Voytek, B. Inferring synaptic excitation/inhibition balance from field potentials. *Neuroimage* **158**, 70–78 (2017).

[8] Donoghue, T. *et al.* Parameterizing neural power spectra into periodic and aperiodic components. *Nature neuroscience* **23**, 1655–1665 (2020).

[9] Muthukumaraswamy, S. D. & Liley, D. T. 1/f electrophysiological spectra in resting and drug-induced states can be explained by the dynamics of multiple oscillatory relaxation processes. *NeuroImage* **179**, 582–595 (2018).

[10] Molina, J. L. *et al.* Memantine effects on electroencephalographic measures of putative excitatory/inhibitory balance in schizophrenia. *Biological Psychiatry: Cognitive Neuroscience and Neuroimaging* **5**, 562–568 (2020).

[11] Akbarian, F. *et al.* The spectral slope as a marker of excitation/inhibition ratio and cognitive functioning in multiple sclerosis. *Human Brain Mapping* **44**, 5784–5794 (2023).

[12] Chini, M., Pfeffer, T. & Hanganu-Opatz, I. An increase of inhibition drives the developmental decorrelation of neural activity. *Elife* **11**, e78811 (2022).

[13] Martínez-Cañada, P. *et al.* Combining aperiodic 1/f slopes and brain simulation: An eeg/meg proxy marker of excitation/inhibition imbalance in alzheimer's disease. *Alzheimer's & Dementia: Diagnosis, Assessment & Disease Monitoring* **15**, e12477 (2023).

[14] He, B. J., Zempel, J. M., Snyder, A. Z. & Raichle, M. E. The temporal structures and functional significance of scale-free brain activity. *Neuron* **66**, 353–369 (2010).

[15] Racz, F. S. *et al.* Separating scale-free and oscillatory components of neural activity in schizophrenia. *Brain and behavior* **11**, e02047 (2021).

[16] Becker, R., Van De Ville, D. & Kleinschmidt, A. Alpha oscillations reduce temporal long-range dependence in spontaneous human brain activity. *Journal of Neuroscience* **38**, 755–764 (2018).

[17] Jensen, O. & Mazaheri, A. Shaping functional architecture by oscillatory alpha activity: gating by inhibition. *Frontiers in human neuroscience* **4**, 186 (2010).

[18] Shirhatti, V., Borthakur, A. & Ray, S. Effect of reference scheme on power and phase of the local field potential. *Neural computation* **28**, 882–913 (2016).

[19] Barry, R. J., Clarke, A. R., Johnstone, S. J., Magee, C. A. & Rushby, J. A. Eeg differences between eyes-closed and eyes-open resting conditions. *Clinical neurophysiology* **118**, 2765–2773 (2007).

[20] Pellegrino, G. *et al.* How cerebral cortex protects itself from interictal spikes: The alpha/beta inhibition mechanism. *Human brain mapping* **42**, 3352–3365 (2021).

[21] Carvalhaes, C. & De Barros, J. A. The surface laplacian technique in eeg: Theory and methods. *International Journal of Psychophysiology* **97**, 174–188 (2015).

[22] Mandelbrot, B. B. & Van Ness, J. W. Fractional brownian motions, fractional noises and applications. *SIAM review* **10**, 422–437 (1968).

[23] Yamamoto, Y. & Hughson, R. L. Coarse-graining spectral analysis: new method for studying heart rate variability. *Journal of Applied Physiology* **71**, 1143–1150 (1991).

[24] Yamamoto, Y. & Hughson, R. L. Extracting fractal components from time series. *Physica D: Nonlinear Phenomena* **68**, 250–264 (1993).

[25] Racz, F. S. *et al.* Multiple-resampling cross-spectral analysis: an unbiased tool for estimating fractal connectivity with an application to neurophysiological signals. *Frontiers in Physiology* **13**, 817239 (2022).

[26] Eke, A., Herman, P., Kocsis, L. & Kozak, L. Fractal characterization of complexity in temporal physiological signals. *Physiological measurement* **23**, R1 (2002).

[27] Nagy, Z., Mukli, P., Herman, P. & Eke, A. Decomposing multifractal crossovers. *Frontiers in Physiology* **8**, 271083 (2017).

[28] Czoch, A. *et al.* Resting-state fractal brain connectivity is associated with impaired cognitive performance in healthy aging. *GeroScience* **46**, 473–489 (2024).

[29] Voytek, B. *et al.* Age-related changes in 1/f neural electrophysiological noise. *Journal of neuroscience* **35**, 13257–13265 (2015).

[30] Dave, S., Brothers, T. & Swaab, T. 1/f neural noise and electrophysiological indices of contextual prediction in aging. *Brain research* **1691**, 34–43 (2018).

[31] Pathania, A. *et al.* Resting eeg spectral slopes are associated with age-related differences in information processing speed. *Biological Psychology* **168**, 108261 (2022).

[32] McFarland, D. J., McCane, L. M., David, S. V. & Wolpaw, J. R. Spatial filter selection for eeg-based communication. *Electroencephalography and clinical Neurophysiology* **103**, 386–394 (1997).

[33] Yao, D. *et al.* A comparative study of different references for eeg spectral mapping: the issue of the neutral reference and the use of the infinity reference. *Physiological measurement* **26**, 173 (2005).

[34] Lei, X. & Liao, K. Understanding the influences of eeg reference: a large-scale brain network perspective. *Frontiers in neuroscience* **11**, 205 (2017).

[35] Kozhemiako, N. *et al.* Sources of variation in the spectral slope of the sleep eeg. *eneuro* **9** (2022).

[36] Perrin, F., Bertrand, O. & Pernier, J. Scalp current density mapping: value and estimation from potential data. *IEEE Transactions on biomedical engineering* 283–288 (1987).

[37] Kantelhardt, J. W., Koscielny-Bunde, E., Rego, H. H., Havlin, S. & Bunde, A. Detecting long-range correlations with detrended fluctuation analysis. *Physica A: Statistical Mechanics and its Applications* **295**, 441–454 (2001).

[38] Chen, Z., Ivanov, P. C., Hu, K. & Stanley, H. E. Effect of nonstationarities on detrended fluctuation analysis. *Physical review E* **65**, 041107 (2002).

[39] Kristoufek, L. Mixed-correlated arfima processes for power-law cross-correlations. *Physica A: Statistical Mechanics and its Applications* **392**, 6484–6493 (2013).

[40] Echeverria, J., Rodriguez, E., Aguilar-Cornejo, M. & Alvarez-Ramirez, J. Linear combination of power-law functions for detecting multiscaling using detrended fluctuation analysis. *Physica A: Statistical Mechanics and its Applications* **460**, 283–293 (2016).

[41] Chiarion, G., Sparacino, L., Antonacci, Y., Faes, L. & Mesin, L. Connectivity analysis in eeg data: a tutorial review of the state of the art and emerging trends. *Bioengineering* **10**, 372 (2023).

[42] van den Broek, S. P., Reinders, F., Donderwinkel, M. & Peters, M. Volume conduction effects in eeg and meg. *Electroencephalography and clinical neurophysiology* **106**, 522–534 (1998).

[43] Krause, B., Márquez-Ruiz, J. & Kadosh, R. C. The effect of transcranial direct current stimulation: a role for cortical excitation/inhibition balance? *Frontiers in human neuroscience* **7**, 602 (2013).

[44] Lányi, O. *et al.* Excitation/inhibition imbalance in schizophrenia: a meta-analysis of inhibitory and excitatory tms-emg paradigms. *Schizophrenia* **10**, 56 (2024).

[45] Eke, A., Hermán, P. & Hajnal, M. Fractal and noisy cbv dynamics in humans: influence of age and gender. *Journal of Cerebral Blood Flow & Metabolism* **26**, 891–898 (2006).

[46] Herman, P., Sanganahalli, B. G., Hyder, F. & Eke, A. Fractal analysis of spontaneous fluctuations of the bold signal in rat brain. *Neuroimage* **58**, 1060–1069 (2011).

[47] Bazanova, O. & Vernon, D. Interpreting eeg alpha activity. *Neuroscience & Biobehavioral Reviews* **44**, 94–110 (2014).

[48] Takei, Y. *et al.* The inhibition/excitation ratio related to task-induced oscillatory modulations during a working memory task: a multtimodal-imaging study using

meg and mrs. *Neuroimage* **128**, 302–315 (2016).